Mussel-Inspired Polydopamine Modification of Bamboo Fiber and Its Effect on the Properties of Bamboo Fiber/Polybutylene Succinate Composites

Gonghua Hong,[a,b,c] Yang Meng,[a,b,c] Zexun Yang,[a,b,c] Haitao Cheng,[d]
Shuangbao Zhang,[a,b,c,]* and Wei Song [a,b,c,]*

A bio-inspired approach to coating polydopamine (PDA) onto bamboo fiber (BF) was developed to enhance the poor interfacial bonding of BF/polybutylene succinate (PBS) biocomposites. The macroscopic features, functional groups, nanoscale topography, and crystallinity of the PDA-coated BF (D-BF) were investigated with digital photography, Fourier transform infrared (FTIR) spectroscopy, atomic force microscopy (AFM), and X-ray diffraction (XRD), respectively. The effects of the PDA loading rate on the performance of the D-BF/PBS biocomposites were also evaluated through the mechanical properties tests, differential scanning calorimetry (DSC), thermogravimetric analysis (TGA), dynamic mechanical analysis (DMA), and scanning electron microscopy (SEM). Treating BF with an optimum concentration of dopamine (DOPA) decreased the polarity of the bamboo fiber, while maintaining the crystal structure of the cellulose. The thermal stability, mechanical properties, and storage modulus of the D-BF/PBS biocomposites were noticeably enhanced because of the good interfacial compatibility. Moreover, the glass transition temperature (T_g) and crystallinity of the biocomposites increased with higher DOPA loading rates. The best properties were observed with a DOPA concentration of 1.0 mg/mL. These findings exhibited the feasibility for the application of PDA in the biomass fiber-reinforced biodegradable polymer composites industry.

Keywords: Bamboo fiber; Polybutylene succinate; Composites; Polydopamine; Surface treatment; Interfacial compatibility; Bio-inspiration

*Contact information: a: MOE Key Laboratory of Wooden Material Science and Application, College of Materials Science and Technology, Beijing Forestry University, Beijing 100083, China; b: Beijing Key Laboratory of Wood Science and Engineering, College of Materials Science and Technology, Beijing Forestry University, Beijing 100083, China; c: MOE Engineering Research Center of Forestry Biomass Materials and Bioenergy, College of Materials Science and Technology, Beijing Forestry University, Beijing 100083, China; d: Department of Biomaterials, International Center for Bamboo and Rattan, Beijing 100102, China; *Corresponding authors: shuangbaozhangj5@163.com (S. Zhang); j5international@163.com (W. Song)*

INTRODUCTION

Recently, energy shortages and environmental pollution have become a common human concern. For conventional plastics, such as PP, PE, PVC, *etc*., decomposing the ever-increasing amount of waste not only consumes a lot of energy, but also produces huge amounts of greenhouse gases (Matkó *et al*. 2005; Koronis *et al*. 2013). To combat these serious problems, a large number of biodegradable polymers, including polylactic acid (PLA), polybutylene succinate (PBS), polybutyleneadipate-co-terephthalate (PBAT), and polyhydroxybutyrate (PHB), have been exploited. However, their high prices limit their marketability (Thakur *et al*. 2014; Moustafa *et al*. 2017). Fortunately, natural fibers derived from biomass resources have advantages, such as high strength, low cost, and being environmentally friendly, which makes them capable fillers to reinforce plastics, as well as reduce costs (Chen *et al*. 2017a; Gao *et al*. 2017; Guo 2017; Yao *et al*. 2017). Therefore, developing a biodegradable biocomposite that is polymerized by biodegradable polymers and natural fibers has attracted increasing attention. Polybutylene succinate (PBS) is a biodegradable polymer used in industrial applications. It can be obtained by the polycondensation of succinic acid and butanediol under certain conditions (Lee *et al*. 2005; Kim *et al*. 2006; Li *et al*. 2015). However, pure PBS has a poor mechanical strength and other inadequate properties, which restrict its applications. Many studies have focused on the use of organic and inorganic fibers including jute (Liu *et al*. 2009), basalt (Zhang *et al*. 2012), and carbon fibers (Liang *et al*. 2015) to enhance the properties of PBS. Considering the full biodegradation performance, biomass fibers excel in this application (Koronis *et al*. 2013; Hassaini *et al*. 2017). Among the diverse biomass fibers, bamboo fiber has been widely used to reinforce various plastics because of its high mechanical strength with a small microfibrillar angle (approximately 2° to 10°) (Tang *et al*. 2015; Liu *et al*. 2016). Moreover, the fast growth of raw bamboo makes it easy to obtain (Haddou *et al*. 2016). However, to date, studies on using bamboo fiber to prepare PBS-based composites have rarely been conducted.

Because hydroxyl groups exist in cellulose and hemicellulose, bamboo fiber possesses a strong polar and hydrophilic surface, which is in opposition to the nonpolar and hydrophobic PBS matrix (Lee *et al*. 2016). Hence, a frail adhesion is formed because of the incompatibility of these two components. This poor interfacial interaction between bamboo fiber and PBS leads to overall inferior performances of the composites, which hinders the use of its products in engineering fields. In order to obtain high-performance biodegradable biocomposites, enhancing the interfacial compatibility between bamboo fiber and PBS was the primary expectation of the present research. Because of the low prices, a large number of modifiers, such as silane (Haddou *et al*. 2016), alkaline (Zhang *et al*. 2015), acetylation (Xu *et al*. 2016), and maleated coupling agents (Ren *et al*. 2017), are used to decrease the polarity of bamboo fiber through surface modification. These modifiers improve the interfacial bonding of bamboo fiber and polymer matrix to some extent, but it is at the expense of decreasing the original mechanical properties of the raw bamboo fiber. This is because the modifiers ruin the bamboo fiber structure itself. Additionally, the treatment processes always react in the solvents, which leaves plenty of spent liquors containing acidic, alkaline, or toxic organic compounds that could ultimately contaminate the environment. Therefore, finding an effective, nonhazardous, biodegradable, and environmentally friendly surface modification of bamboo fiber is urgent.

Fortunately, the tissues and organs of animals and plants provide inspiration for the preparation of functional materials. The adhesive system of marine mussels, which have super strong adhesion, has received great interest in recent years. It was found that 3,4-dihydroxyphenyl-1-alanine (DOPA), the primary functional element of mussel adhesive proteins (MAPs), could adhere to the surfaces of various materials *via* polydopamine (PDA) formed by oxidative self-polymerization (Deming 1999; Lin *et al*. 2007; Waite 2008). The chemical versatility and protein diversity of catechol groups in PDA can establish sophisticated bond formations through hydrogen bonds, quinhydrone charge-transfer complexes, and chelation, which gives PDA its strong adhesive ability so that it can adhere to almost any solid material surface (Yang *et al*. 2011; Matos-Pérez *et al*. 2012; Gu *et al*. 2013). Inspired by the structure of DOPA, researchers have synthesized PDA-modified materials with the same functional unit that is in MAPs. As for fiber-reinforced polymer composites, the catechol groups in DOPA form hydrogen bonds with fibers, while the C-H chains are wrapped with polymer matrix, which can improve the fiber-matrix adhesion of composites (Ji *et al*. 2016). Luo *et al*. (2016) used PDA to improve the dispersion and interfacial interaction between halloysite nanotubes (HNTs) and PLLA matrix, and the mechanical properties and compatibility of the HNTs/PLLA composites were improved. Yuan *et al*. (2017) introduced bio-inspired PDA to hybrid Nomex/PTFE fabric and demonstrated that the tensile and bonding strengths of the amino-functionalized fabric composites were noticeably superior to that of the non-treated composites. Additionally, the surface compatibility between the polymer matrix and carbon nanotube (Wan *et al*. 2015), silica fiber (Wang *et al*. 2011), and other fillers was also promoted by treatment with DOPA. Although some researchers have focused on the interfacial crystallization of PDA-coated continuous ramie fibers and hemp fiber/polymer composites, using PDA to coat short-staple natural fibers in order to enhance plastic composites has rarely been studied, especially for bamboo fiber (Bourmaud *et al*. 2009; Zhou *et al*. 2014a,b). Furthermore, PDA can be obtained in a way that is mild, green, and harmless. According to previous studies, PDA can be easily obtained by self-polymerization in an aqueous dopamine solution at a pH of 8.5 without the use of extra toxic reagents (Lee *et al*. 2007).

The objective of this study was to use a bio-based modifier, PDA, to improve the interfacial compatibility between the surface of bamboo fiber and PBS. In this work, bamboo fiber was first treated in aqueous dopamine hydrochloride according to the typical method given in Lee *et al*. (2007). PDA-coated bamboo fiber (D-BF)/PBS biocomposites were fabricated *via* compression molding. The macroscopic features, functional groups, nanoscale topography, and crystallinity of the D-BF were investigated through digital photography, Fourier transform infrared (FTIR) spectroscopy, atomic force microscopy (AFM), and X-ray diffraction (XRD), respectively. Meanwhile, the effects of the dopamine concentration on the dispersion of D-BF in the PBS matrix, crystallinity of the resin matrix, and the mechanical properties, thermal stability, and dynamic mechanical analysis of the ultimate PBS-based biocomposites were comprehensively evaluated. The bio-inspired approach in this study showed promising potential for compatibilizer applications in biomass fiber-reinforced biodegradable plastic composites as an alternative to traditional modifiers.

EXPERIMENTAL

Materials

Bamboo fiber with a mixed particle size of 40-to 60-mesh and fiber length below 380 μm was supplied by Anhui Sentai WPC New Material Co. Ltd (Huzhou, China). The PBS (flow index = 2.0 g/10 min, crystallinity = 32%, and density = 1.24 g/cm^3), from Showa Highpolymer Co. Ltd (Tokyo, Japan), was used in this study as the polymer matrix. Dopamine hydrochloride (98.5%) and tris(hydroxymethyl) methyl aminomethane (tris-HCl) (99.9%) were purchased from Solarbo Life Sciences Co. Ltd. (Beijing, China). Other chemicals, including hydrochloric acid, solid paraffin, and deionized water, were purchased from Beijing Chemical Reagents (Beijing, China). All of the materials were used without further purification.

Treatment of the Bamboo Fiber with Polydopamine (PDA)

Bamboo fiber was first dried in an air-dry oven at 80 °C for 48 h, and then it was treated in a dopamine hydrochloride solution with different dopamine concentrations (0.5, 1.0, 1.5, 2.0, and 2.5 mg/mL). The tris-HCl buffer solution was added to the mixed solutions to adjust the pH to approximately 8.5. Next, the mixed solutions were stirred at 300 r/min and room temperature for 48 h. It was observed that, after self-polymerization of the dopamine, the color of the mixed solutions changed from colorless to dark brown. After the last process, the treated bamboo fiber was obtained by filtering, and then the PDA, which was not yet coated onto the fiber, was washed several times with distilled water until the solutions became clear. Finally, PDA-coated bamboo fiber was obtained by drying it in a vacuum oven at 80 °C for 48 h. The labels of the control and experimental groups with bamboo fiber treated with different concentrations of dopamine are shown in Table 1.

Table 1. Labels of the Control and Experimental Groups

Label	DOPA Solution Concentration (mg/mL)	BF/D-BF (wt.%)	PBS (wt.%)	Other Additives (wt.%)	V_f
Control	0	49	49	2	0.5
D-BF-1	0.5	49	49	2	0.5
D-BF-2	1.0	49	49	2	0.5
D-BF-3	1.5	49	49	2	0.5
D-BF-4	2.0	49	49	2	0.5
D-BF-5	2.5	49	49	2	0.5

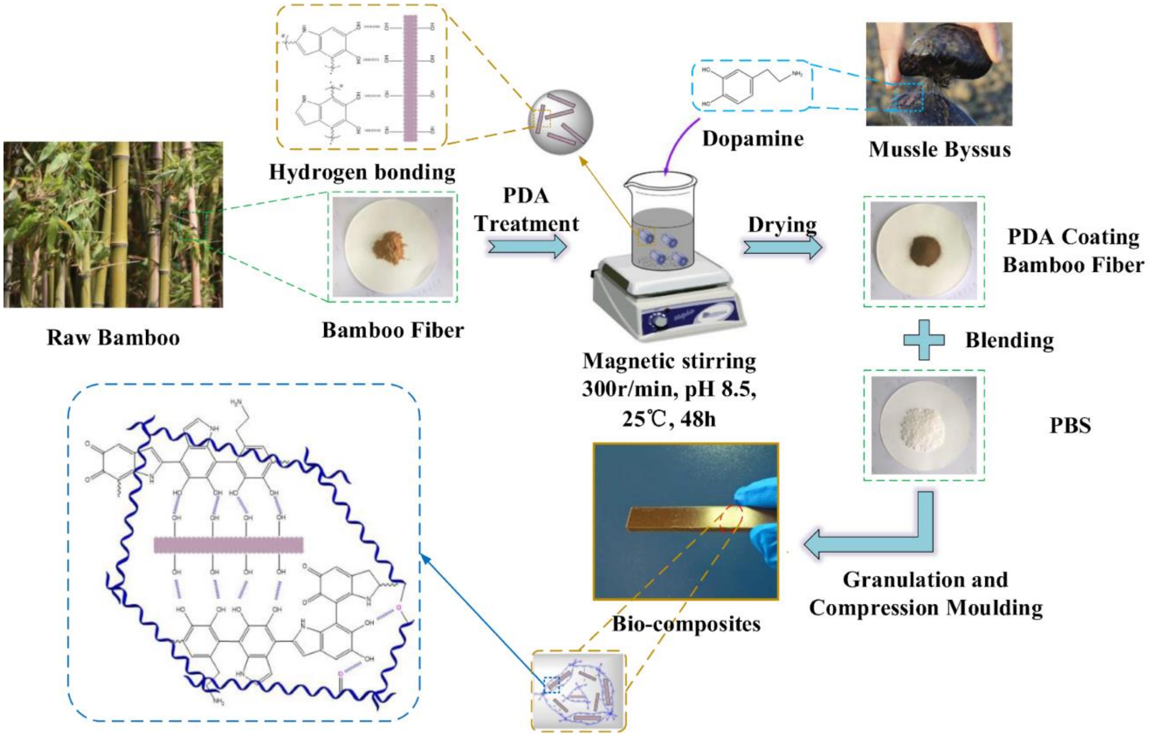

Fig. 1. Schematic of the preparation of PBS-based biocomposites reinforced with PDA surface treated bamboo fiber

Preparation of the Bamboo Fiber/PBS Composites

The process for the preparation of the bamboo fiber/PBS composites (Fig. 1) was similar to that described previously (Song *et al*. 2015). The composites were prepared with 49 wt.% bamboo fiber and 49 wt.% PBS. These two components were first mixed in a high-speed blender at approximately 2900 rpm for 5 min. The mixture was dried in an oven at 103 °C for 2 h. Then, the mixture was extruded *via* a co-rotating twin-screw extruder (KESUN KS-20, Kunshan, China) with a screw diameter of 20 mm and length-to-diameter ratio of 36:1. The corresponding temperature profile along the extruder barrel was 135/140/145/145/135 °C, and the screw speed of the equipment was 180 rpm. The mixtures were ground until the diameter of the particles was 2 mm. Next, the processed particles were dried in an oven at 103 °C for another 2 h and taken out for hand matting. The composites were produced with a hot press (SYSMEN-II, China Academy of Forestry, Beijing, China) at 145 °C and a pressure of 4 MPa for 6 min. The density of the PBS composites was 1.28 g/cm^3, and the dimensions were 270 × 270 × 4 mm. The formed mat was cooled down at 4 MPa and room temperature for 6 min before demolding. Finally, according to the related standards for the tests, all of the mats were cut to the required dimensions. The labels of the PBS-based biocomposites obtained from the untreated and PDA-coated bamboo fibers are the same as the labels shown in Table 1.

Characterization of the Bamboo Fiber

Fourier transform infrared (FTIR) spectroscopy preparation and analysis

The variations in the functional groups of the untreated and PDA-coated bamboo fibers were analyzed by FTIR analysis (Bruker Vertex 70v, Karlsruhe, Germany). Before recording the spectra, the BF samples were mixed with potassium bromide (KBr) at a weight ratio of 1:100. All of the spectra were displayed at a scanning range of 4000 to 500 cm^{-1} with 40x scans at a resolution of 4 cm^{-1}. Each group was measured three times to eliminate any error.

X-ray diffraction (XRD) procedure and analysis

The crystallization property of the PDA-coated and untreated bamboo fiber samples was analyzed by XRD analysis. The bamboo fiber samples were analyzed on a D8 Advance X-ray diffractometer (Bruker AXS). The X-ray beam was Cu Kα (λ = 1.542 Å) radiation. The operation was carried out at 40 kV and 30 mA, and the scanning range (2θ) was from 0° to 40° with a step size of 5°/min. The crystallization index was calculated with Eq. 1,

$$CI\% = (A_c \ / \ A_a) \times 100 \tag{1}$$

where A_c is the peak area (a.u.•°), and A_a is the area above the baseline of the entire area (a.u.•°). The peaks, which were calculated as Peaks (002), crystalline reflection, and total diffractive part were determined with JADE software (MDI JADE 5.0, Material Data, Inc., Livermore, CA, USA) (Gao *et al*. 2016).

Nanoscale surface topography and roughness analysis

The nanostructures of the PDA, untreated bamboo fiber, and PDA-coated bamboo fiber were investigated with a Multimode 8 AFM (Bruker) using the tapping mode under atmospheric conditions. To obtain the two-dimensional (2D) and three-dimensional (3D) topographies, roughness, and PDA nanoparticle sizes, the results were further analyzed with NanoScope Analysis software (Bruker).

Characterization of the Bamboo Fiber/PBS Composites

Mechanical property test

The flexural tests of the bamboo fiber/PBS composites that had been treated with different concentrations of PDA were carried out according to ASTM D790-03 (2003). The tests were operated in an electronic universal testing machine (Changchun Kexin Instrument Equipment Co. Ltd., Changchun, China) at a testing speed of 2 mm/min, and the span between the two fulcrums was 64 mm. The dimensions of each sample were 80 × 13 × 4 mm.

The tensile tests were carried out according to ASTM D638-03 (2003) on an electronic universal testing machine at a testing speed of 2 mm/min, same as for the flexural tests. The sample dimensions were 160 × 20 × 4 mm. The samples were dumbbell-shaped with a radius of arc of 76 mm, gauge length of 50 mm, and middle part width of 13 mm.

The impact tests were carried out according to ASTM D256-03 (2003) on a cantilever beam impact tester (Chengde Precision Testing Machine Co. Ltd., Chengde, China) with an impact energy of 2 J. The sample dimensions were 80 × 10 × 4 mm, and the moment of force of the pendulum bob was 1.7717 Nm. Eight replicates were used in the flexural, tensile, and impact tests, and the average values were calculated to reflect the measurement results.

Thermal property test

The melting temperature and crystallization properties of the composites were tested by differential scanning calorimetry (DSC) analysis (Netzsch DSC-204, Germany). To eliminate the thermal history, the samples first underwent an up-down temperature recycling from room temperature to 180 °C, and then these samples were heated to 180 °C again at a constant heating rate of 10 °C/min with an argon flow rate of 50 mL/min. A sample of approximately 6 ± 0.02 mg was placed in an aluminum pan.

The thermal stability properties of the composites were investigated with a TA 309F3 thermogravimetric analysis (TGA) device (TA Instruments, New Castle, DE, USA). The test results were obtained by heating the samples from room temperature to 600 °C at the same conditions used for the DSC analysis.

Dynamic mechanical analysis (DMA)

Samples were tested with a dynamic thermomechanical analyzer (TA Instruments) in the single cantilever mode. The sample dimensions were 35 × 10 × 3 mm, the scanning frequency was 1 Hz, and the heating rate was 3 °C/min. The test temperature ranged from -80 to 100 °C. All of the samples were tested three times to avoid errors.

The adherence factor (*A*) was used to assess the interface bonding between the fiber and plastic matrix, and was calculated with Eq. 2 (Kubát *et al*. 1990),

$$A(\mathrm{MPa}) = \left(1/(1 - V_\mathrm{f})\right)\left(\tan\delta_\mathrm{c}/\tan\delta_\mathrm{m}\right) - 1 \tag{2}$$

where the subscripts *c* and *m* represent the biocomposite and plastic matrix, respectively, and V_f is the fiber volume fraction (a.u.). Lower *A* values are in accordance with a better interface compatibility and *vice versa* (Li *et al*. 2017).

Water absorption test

The water absorption (WA) test was conducted in consistent with the research by Liu *et al*. (2014). The oven-dry square samples with 50 × 50 × 4 mm^3 were completely immersed in distilled water at 20 ± 2 °C for 12 days. At intervals of 24 h, samples were weighed after removal of excessive water on the surface. Five specimens were tested and the average values were recorded to represent the results. The water absorption at 24 h intervals were calculated with Eq. 3,

$$\mathrm{WA} = (w_2 - w_1) / w_1 \times 100\% \tag{3}$$

where w_1 is the oven-dry weight of the initial samples and w_2 is the average weight of samples at predetermined intervals.

Scanning electron microscopy (SEM)

The impact fracture morphology of the biocomposites was analyzed by a FEI scanning electron microscope (Quanta FEG, Thermo Fisher Scientific Inc., Waltham, MA, USA) with an acceleration voltage of 15 kV. The samples were soaked and fractured in liquid nitrogen to obtain an excellent interface. The samples were sputter-coated with gold before observation.

RESULTS AND DISCUSSION

Chemical Composition and Surface Morphologies of the Untreated and PDA-Coated Bamboo Fibers

Macroscopic features of the untreated and PDA-coated bamboo fibers

Figure 2 shows photographs of the untreated and PDA-coated bamboo fibers. The untreated bamboo fiber exhibited a light-yellow color. The color of the PDA-coated bamboo fiber became darker because of the oxidative self-polymerization of dopamine, which displayed the same phenomenon that was seen for the coating of PDA onto ramie fiber (Zhou *et al*. 2014a,b). With an increased dopamine concentration, more PDA particles were loaded onto the surface of the bamboo fiber, and thus a black dopamine film was formed. When the black film became thicker, the color of the bamboo fiber changed from light brown to black.

Fig. 2. Photographs of the untreated and PDA-coated bamboo fibers; A: Control; B: D-BF-1; C: D-BF-5

FTIR spectroscopy analysis

The FTIR spectra of the untreated bamboo fiber (control) and PDA-coated bamboo fiber (D-BF-1, D-BF-5) are shown in Fig. 3. In order to demonstrate the impact of the PDA loading rate on the bamboo fiber more accurately, the absorbance-FTIR spectra attribution results were used to analyze the chemical compositions at the same baseline level, which can easily find variations in the contents of functional groups. The important positions and potential structure assignments of the peaks correlating with the PDA and bamboo fiber are listed in Table 2.

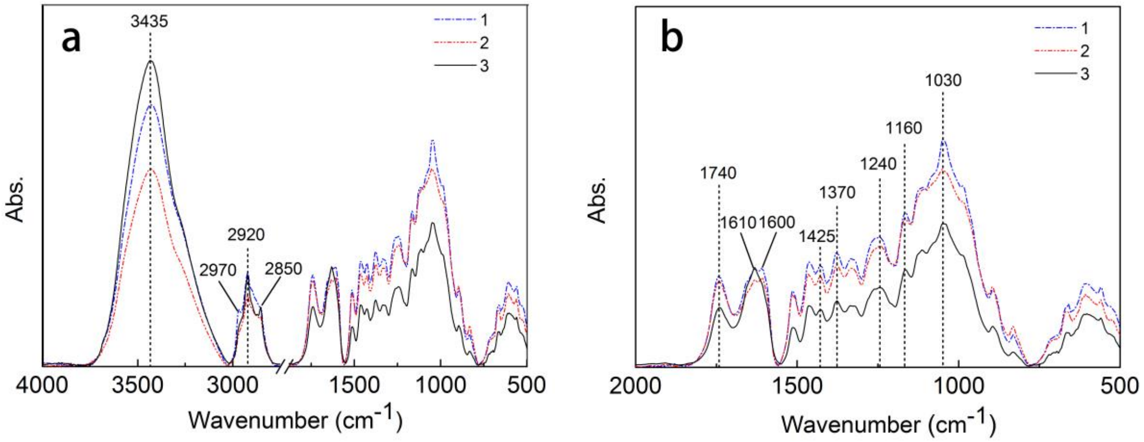

Fig. 3. FTIR spectra of the untreated and PDA-coated bamboo fibers; a: whole region spectra; b: fingerprint region spectra; (1) Control; (2) D-BF-1; (3) D-BF-5

Table 2. Infrared Absorbance Peaks of the PDA and Bamboo Fiber Constituents

Wavenumber (cm^{-1})	Potential Functional Groups
3200 - 3500	Hydroxyl (-OH) stretching vibration (cellulose, hemicellulose, lignin, and PDA); amino (-NH) stretching vibration (PDA)
3000 - 2842	Methyl (-CH_3), methylene (-CH_2-) stretching vibration
1740	Carbonyl (C=O) stretching vibration (hemicellulose)
1610 - 1600	Carbon skeleton stretching of benzene ring (lignin and PDA); amino (-NH) bending vibration (PDA)
1425	Methylene (-CH_2-) shear vibration (cellulose)
1370	C-H bending vibration (cellulose and hemicellulose)
1240	Acyl-oxygen (CO-OR) stretching vibration (hemicellulose); benzene-oxygen bond stretching vibration (lignin);
1160	C-O-C stretching vibration (cellulose and hemicellulose)
1030	Aromatic ether (C–O) and secondary alcohols stretching vibration (cellulose, hemicellulose, and lignin)

Figure 3 shows the comparison of the FTIR spectra obtained for the untreated bamboo fiber and bamboo fiber subjected to different dopamine concentrations. Compared with the untreated bamboo fiber in Fig. 3a, the absorbance intensity of the characteristic peak near 3435 cm^{-1}, which was designated as the stretching vibration of amino (-NH) and hydroxyl (-OH) groups, showed a distinct difference (Gu *et al*. 2013; Tang *et al*. 2015). During treatment with the dopamine solution, the benzene-OH group in the PDA molecules formed hydrogen bonds with the free hydroxyl groups on the surface of the bamboo fiber, which reduced the number of free hydroxyl groups both in the bamboo fiber and PDA molecules (curve 2). When the bamboo fiber was treated with a high concentration of dopamine, the overloading of PDA exposed numerous free hydroxyl groups because of a lack of hydrogen bonds, and consequently, the strongest characteristic peak appeared (curve 3). The characteristic peaks located at 1740, 1425, 1370, and 1160 cm^{-1} in Fig. 3b were assigned to C=O stretching vibration, -CH_2- shear vibration, C-H bending vibration, and C-O-C stretching vibration, respectively (Zhang *et al*. 2015). These four peaks are characteristic of cellulose and hemicellulose. As the PDA loading rate increased, the absorption intensity of these peaks showed a downward trend, but the relative content remained unchanged. This result was probably because of the increased PDA film thickness, which gave the bamboo fiber a "black coat" (Fig. 2). The "black coat" reduced the intensity of light transmitted to the surface of the bamboo fiber, which caused the characteristic peaks of cellulose and hemicellulose to simultaneously decrease. The peaks near 2920 cm^{-1} were attributed to the stretching vibration of methyl ($-CH_3$) and methylene ($-CH_2-$) in both the bamboo fiber and PDA molecules (Chen *et al*. 2017a; Zhou *et al*. 2014a). For the untreated bamboo fiber, there existed a weak peak at 2970 cm^{-1}, which was attributed to the antisymmetric stretching vibration of $-CH_3$. When the bamboo fiber was treated with PDA, the weak peak of $-CH_3$ was hidden because of the increased methylene group (2970 cm^{-1}) content, and at the same time, a weak new peak at 2850 cm^{-1} appeared, which was assigned to the symmetrical stretching vibration of $-CH_2-$ in the PDA molecules. Although the "black coat" decreased the FTIR spectra intensity of the bamboo fiber, the absorbance intensity peaks of the methylene group at 2920 and 2850 cm^{-1} mainly produced by the PDA molecules still increased with a high content of PDA. The peaks located near 1600 cm^{-1} that were assigned to the carbon skeleton vibration of lignin were disturbed because of the similar molecular structure of dopamine (Haddou *et al*. 2016). Additionally, the amino deformation vibration peak located at 1608 cm^{-1} was near the peak at 1600 cm^{-1} (Wang *et al*. 2017), and consequently, the two peaks merged into a new peak that shifted to a higher wavenumber (curve 3). All together, these results demonstrated that the PDA nanoparticles had been successfully coated onto the surface of the bamboo fiber, and the proper loading rate of PDA can decrease the polarity of the surface of the bamboo fiber by diminishing the number of free hydroxyl groups, which indicated that PDA can be used as a coupling agent to improve the interface of bamboo fiber and plastic composites.

XRD analysis

The crystallinity of the cellulose in the bamboo fiber was one of the prominent factors that determined the mechanical properties. Figure 4 exhibits the XRD patterns obtained for the untreated bamboo fiber and bamboo fiber treated with different concentrations of dopamine.

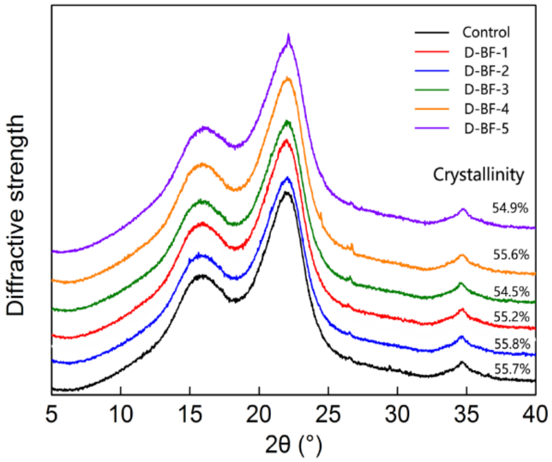

Fig. 4. XRD patterns of the untreated bamboo fiber and bamboo fiber treated with different concentrations of dopamine

As shown in Fig. 4, the XRD pattern for the untreated bamboo fiber demonstrated the typical crystalline structure of native cellulose I, which possessed (101), (002), and (040) diffraction peaks located at the 2θ angles of 17°, 22.5°, and 35°, respectively (Yao *et al*. 2017). Compared with the untreated bamboo fiber, coating PDA onto the bamboo fiber had little impact on the three typical crystal diffraction peaks of the cellulose with respect to both the shapes and 2θ angles, which indicated that the treatment process can hardly destroy the structure of the crystalline regions in the cellulose chain. Also, the high crystallinity (approximately 55%) was preserved because of the stable hydrogen bonds formed by the cellulose intramolecular hydroxyl groups (Chu *et al*. 2017). Additionally, the loading rate of the PDA had no obvious effects on the crystallinity. The original fiber structure remained unchanged even after the addition of PDA at the highest loading rate (D-BF-5).

As stated above, it was concluded that the mechanism of PDA adhesion was probably generated by the catechol groups in the PDA molecular structure that can form hydrogen bonds with free hydroxyl groups in the bamboo fiber, which was in accordance with the results of the FTIR spectroscopy.

Moreover, these results also illustrated that appropriate PDA can promote the nonpolarity of the surface of the bamboo fiber while maintaining the original mechanical strength. This was its unique advantage compared with other surface modifying methods, such as the alkali, acetic acid, and maleic anhydride grafting treatments, which makes it a promising interface modifier.

Microscopic morphology in atomic force microscopy (AFM)

The microscopic morphology of the PDA particles and the surface topography and roughness of the untreated and PDA-coated bamboo fibers characterized by 2D and 3D AFM images are shown in Fig. 5. As shown in Fig. 5a, the dopamine monomers formed PDA *via* oxidative self-polymerization. The PDA particles were approximately 77 nm in size, which showed that the PDA was a nanomaterial.

Figure 5b showed the surface morphology of the bamboo fiber was smooth and flat with a root-mean-square roughness (R_q) value of 1.61 nm. At the lowest PDA loading rate (D-BF-1), the PDA nanoparticles were easily recognized with a particle size of approximately 81 nm, as can be seen in Fig. 5c, and a distinctly rough surface appeared in the 3D image as the R_q value increased to 5.33 nm.

However, when the bamboo fiber was treated at the highest PDA loading rate (D-BF-5), more PDA nanoparticles composed a thin film coating on the surface of the bamboo fiber, which made the PDA nanoparticles difficult to identify in Fig. 5d. Moreover, compared with the low loading rate, the R_q value decreased to 3.17 nm after the increased addition of PDA nanoparticles, and the surface topography in Fig. 5d became compact and smooth.

These results confirmed that the PDA nanoparticles were loaded onto the surface of the bamboo fiber. Additionally, the PDA loading rate influenced the roughness of the bamboo fiber, which may be a potential factor that affects the bamboo-plastic interface, like the silane coupling agent (Xie *et al*. 2010).

(a) PDA Nanoparticles

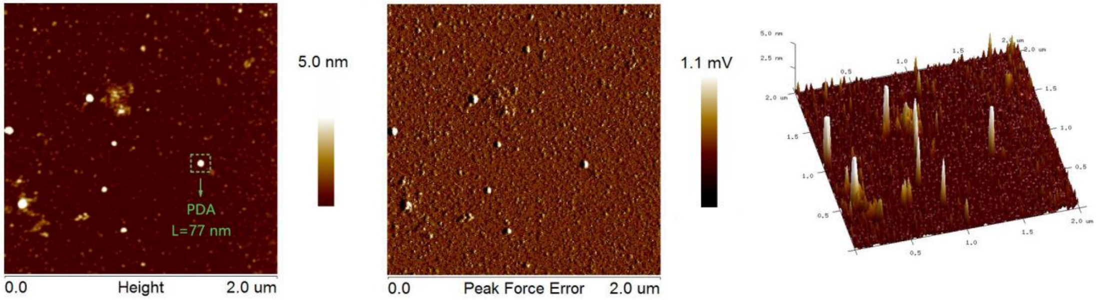

(b) Untreated Bamboo Fibers

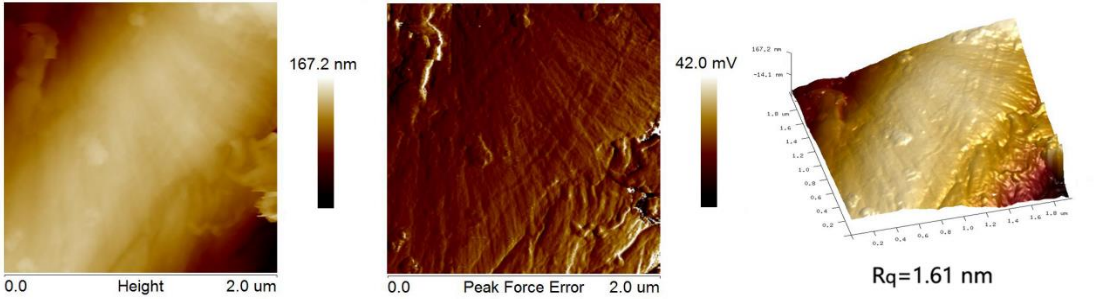

(c) D-BF-1

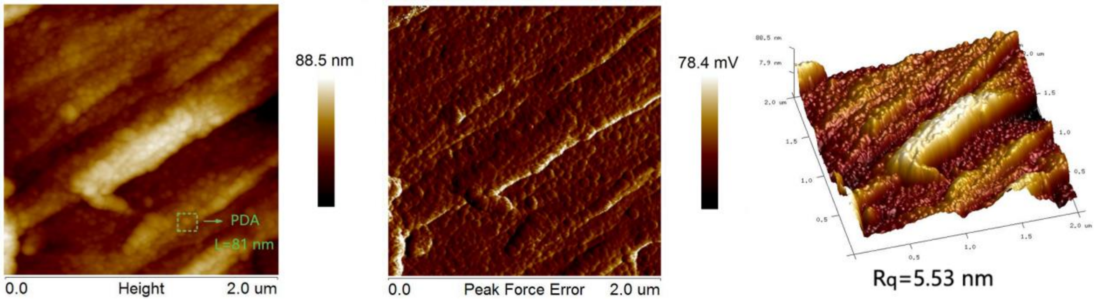

(d) D-BF-5

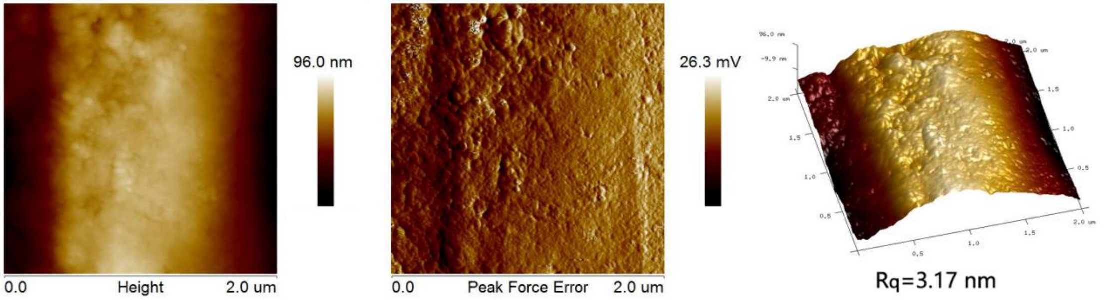

Fig. 5. 2D and 3D AFM images of the microscopic morphologies of (a) PDA nanoparticles, (b) untreated bamboo fiber (control), (c) D-BF-1, and (d) D-BF-5

Characterization of the Bamboo Fiber/PBS Composites

Mechanical properties

The mechanical properties test results of the untreated and PDA-coated bamboo fiber/PBS composites are recorded in Table 3. Compared with the composites made with the untreated bamboo fiber and irrespective of deviations, the flexural strength, flexural modulus, tensile strength, tensile modulus, and impact strength of the groups treated with PDA were wholly improved as the dopamine concentration increased from 0.5 to 2.5 mg/mL, which indicated that PDA can reduce the polarity of the bamboo fiber and promote the interface compatibility between the bamboo fiber and PBS matrix. The PDA nanoparticles had both hydrophilic (-OH, -NH) and hydrophobic (Benzene ring, C-H chain) groups. With the addition of PDA, the PBS matrix molecular chain was twisted together with the benzene ring and C-H chains, while the hydrophilic (-OH, -NH) groups were combined with the bamboo fiber *via* hydrogen bonds. Additionally, the PBS matrix was polymerized by ester groups, which could interact with the -OH groups in the PDA molecules through hydrogen bonds. Therefore, the PDA-coated bamboo fiber/PBS composites demonstrated excellent mechanical properties.

For the PDA-treated composites, with an increasing PDA loading, the mechanical properties of the bamboo fiber/PBS composites displayed the tendency to increase at first, and then decline. The mechanical properties of the composites with a dopamine concentration of 1.0 mg/mL (D-BF-2) reached their maximum values, and were better than those of the other groups in the study, which indicated that the amount of PDA should be moderate. The smallest PDA amount could hardly coat the whole fibers, which resulted in a deficient reaction between the bamboo fiber and PBS matrix. In contrast, the highest PDA amount could generate a thick film and exposed free hydroxyl groups because of the uncoated PDA, which formed a disruptive interfacial sheet that wrapped the surface of the fibers and bonded with the matrix. Additionally, the overloaded PDA nanoparticles also acted as plasticizers, which negatively affected the mechanical properties, especially the impact strength, because of the increasing toughness of the PBS matrix (Zhou *et al*. 2014a). For these conditions, a fragile interface was formed between the matrix and fiber, and thus the mechanical properties of the composites were partly reduced. Consequently, the best dopamine concentration in this study was 1.0 mg/mL (D-BF-2), which caused increases in the flexural strength, flexural modulus, tensile strength, tensile modulus, and impact strength of 34.2%, 23.4%, 65.5%, 41.3%, and 63.4%, respectively, in comparison with the untreated composites.

Table 3. Mechanical Properties of the Untreated and PDA-Coated Bamboo Fiber/PBS Composites

Label	Flexural strength (MPa)	Flexural modulus (GPa)	Tensile strength (MPa)	Tensile modulus (GPa)	Impact strength (kJ/m^2)
Control	31.38(0.67)^d	2.05(0.13)^e	13.62(1.15)^e	0.75(0.18)^d	10.25(1.11)^e
D-BF-1	37.06(0.41)^{bc}	2.41(0.55)^b	18.67(0.27)^c	0.85(0.11)^c	14.63(1.35)^{bc}
D-BF-2	42.14(0.78)^a	2.53(0.09)^a	22.54(0.56)^a	1.06(0.17)^a	16.75(2.36)^a
D-BF-3	38.88(1.57)^b	2.38(0.14)^{bc}	20.46(1.37)^b	1.03(0.09)^{ab}	15.33(1.60)^b
D-BF-4	35.28(0.99)^c	2.33(0.24)^{cd}	19.32(0.64)^{bc}	0.95(0.17)^b	14.25(1.02)^c
D-BF-5	34.72(0.82)^c	2.26(0.13)^d	16.59(0.97)^d	0.82(0.15)^{cd}	12.15(0.79)^d

Note: The standard deviations of the test results are recorded in parentheses. The statistical differences ($P < 0.05$) are labeled with letters following the parentheses.

Differential scanning calorimetry (DSC) analysis

Figure 6 shows the DSC thermograms of the pure PBS and composites enhanced with bamboo fiber treated with different concentrations of dopamine. Compared with the pure PBS, the melting endothermic peak of the composites shifted to a higher temperature, which indicated that the filling of bamboo fiber into the composites improved the melting temperature (T_m) of the PBS matrix. Bamboo fiber consists of cellulose, hemicellulose, and lignin, which have higher T_m values than PBS (Xu *et al*. 2016). Additionally, the PBS molecular chain became more stable after adding the bamboo fiber. Thus, the bamboo fiber was a helpful factor in hindering the melting of the composites. For the PBS, which has both non-polar and polar groups in the molecular chains, the untreated and PDA-coated bamboo fibers exhibited the same influence on the melting temperature of the PBS, which caused the slightly different T_m values for the experimental and control groups. Furthermore, the addition of the bamboo fiber improved the crystallinity of the PBS, which indicated that the bamboo fiber had a nucleation function because of the high aspect ratios and appropriate particle sizes. Moreover, inducing the formation of transcrystalline features (TC) can improve the crystallinity of the polymer (Zhou *et al*. 2014b). The coating of PDA onto the surface of bamboo fiber can form TC with PBS, and thus the crystallinity of the PDA-BF/PBS composites were significantly enhanced. With increased PDA loading rates on the surface of the bamboo fiber, the concentration of hydrogen bonds between C=O in the PBS chain and free -OH and -NH in the PDA increased, which further improved the nucleation density of the TC in the PBS and increased the crystallinity from 48.12% to 55.67%. The higher crystallinity of the PBS promoted the brittleness of the matrix, which demonstrated that PDA functioned as a plasticizer in accordance with the hypothesis illustrated in the *Mechanical properties* section (pages 8429-8430). Generally, the untreated BF/PBS composites should have had the highest impact strength because of the lower crystallinity. However, the opposite trend was observed, as can be seen in Table 3. This result was attributed to the excellent interface compatibility of the PDA-bamboo fiber and PBS matrix. A compact interface was formed, which improved the continuous transmission of the stress and increased the impact strength (D-BF-2).

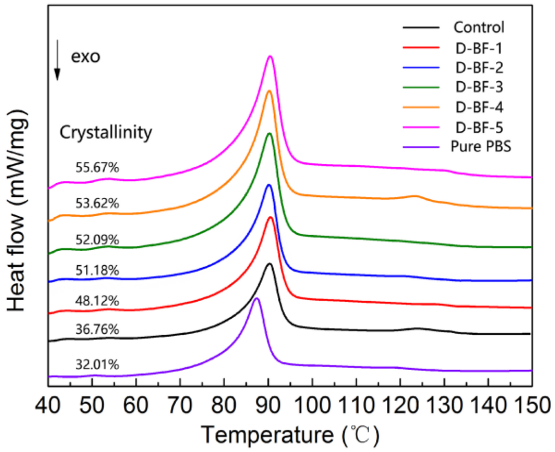

Fig. 6. DSC curves of the pure PBS and bamboo fiber/PBS composites

Thermogravimetric (TG) and differential thermogravimetric (DTG) analysis

Figure 7 shows the thermogravimetric (TG) and differential thermogravimetric (DTG) curves obtained for the PBS matrix composites enhanced with untreated bamboo fiber and bamboo fiber treated with different dopamine concentrations. The comprehensive analysis of the thermal degradation variation, shown in Fig. 7, revealed that during the complete thermal degradation regions from 30 to 600 °C, the pyrolysis of the BF/PBS composites was dividable into three stages. The data of the thermal degradation temperature is reported in Table 4. In stage I (30 to 225 °C), the 5% mass loss was attributed to the evaporation of moisture and depolymerization of macromolecular compounds in the bamboo fiber. In stage II (225 to 382 °C) and stage III (382 to 600 °C), the main pyrolysis of the BF/PBS composites took place with mass losses of approximately 45.80% and 32.13%, respectively. The weight loss of stage II was attributed to the decomposition of cellulose and hemicellulose (Moustafa *et al*. 2017). In particular, the intramolecular hydrogen bonds in the crystal region of the cellulose molecular chain engendered a higher thermal ability, which caused a shift of the DTG curves from 315 to 375 °C. This was in line with the pyrolysis region of pure cellulose (Liu *et al*. 2014). In stage III, the lignin and PBS matrix were completely degraded. Because of the stable structure of the methoxy functional groups in the lignin and the high polymerization degree of the PBS matrix, more energy was required to destroy these two molecular structures, and the highest thermal degradation rate of the whole pyrolysis process occurred during this stage (Li *et al*. 2015; Chen *et al*. 2017a). Above 450 °C, the mass loss was unchanged, leaving residues that were hardly pyrolyzed.

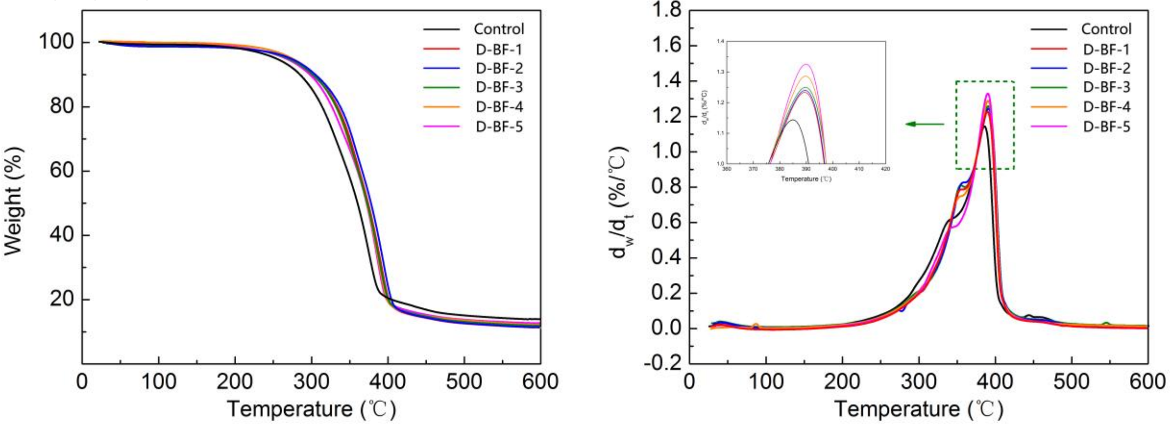

(a) **(b)**

Fig. 7. TGA curves (a) and differential thermogravimetric (DTG) curves (b) of the pure PBS and bamboo fiber/PBS composites

Table 4. Comparison of the Pyrolysis Characteristics of the Pure PBS and Bamboo Fiber/PBS Composites

Labels	Stage I	Stage II			Stage III			
	T_{i1} (°C)	T_{i2} (°C)	T_1 (°C)	T_2 (°C)	T_{i3} (°C)	T_3 (°C)	T_4 (°C)	T_m (°C)
Control	30.0	221.3	329.0	357.4	371.6	378.8	397.1	384.3
D-BF-1	30.0	224.5	323.3	361.3	382.3	382.8	400.5	390.4
D-BF-2	30.0	225.6	333.1	362.3	382.9	384.2	401.2	391.7
D-BF-3	30.0	225.1	332.7	362.0	382.5	383.3	400.5	391.1
D-BF-4	30.0	225.0	332.5	361.7	381.9	383.3	399.3	390.7
D-BF-5	30.0	224.7	331.9	360.1	381.8	383.0	399.0	390.1

Note: T_{i1}, T_{i2}, and T_{i3} represent the initial degradation temperature of Stage I, II, and III, respectively; T_m represents the temperature of the maximum peak in the DTG curve; T_1, T_2, T_3, and T_4 represent the temperatures of the 20%, 40%, 60%, and 80% mass loss rates, respectively.

The initial pyrolysis temperature of the PBS matrix-based composites prepared from the PDA-coated bamboo fiber was higher than that of the control group during the different stages presented in Fig. 7, as well as the 20%, 40%, 60%, and 80% mass loss stages recorded in Table 4. Because of the high thermal stability of PDA, which was oxidative self-polymerized by the dopamine monomer, the PDA film can protect the bamboo fiber from being degraded. This increased the degradation temperature of the PDA-coated bamboo fiber. Furthermore, the addition of PDA improved the interfacial compatibility between the bamboo fiber and PBS matrix, which made the heat transfer more uniform in the composites, and thus thermal stability was promoted. Moreover, the PDA nanoparticles also acted as plasticizers, as was discussed in the *Differential scanning calorimetry (DSC) analysis* section (pages 8430-8431), which increased the crystallinity of the PBS matrix with the catechol groups of the PDA-coated bamboo fiber *via* hydrogen bonds. Therefore, a high depolymerization temperature occurred. The reasons stated above could have explained the excellent thermal stability of the PDA-treated bamboo fiber/PBS composites compared with the control group. However, with an increased dopamine concentration, little difference in the pyrolysis temperature of the experimental groups was exhibited, which suggested that the PDA loading rate mostly did not influence the thermal stability of the PDA-treated bamboo fiber/PBS composites. Unexpectedly, the group treated with a dopamine concentration of 1.0 mg/mL (D-BF-2) displayed a slightly higher degradation temperature than that of the other groups, which was attributed to the better interfacial compatibility, which was in accordance with the mechanical properties and DSC analysis results. When pyrolysis ended, the amount of residue from the control group was lower than that from the experimental groups. This was because the process of coating PDA onto the bamboo fiber occurred in an aqueous solution, which dissolved some of the water-soluble saccharides in the raw bamboo fiber.

DMA

Dynamic mechanical analysis (DMA) was an effective method for evaluating the interfacial interaction between the bamboo fiber and PBS matrix. The temperature dependence of the storage modulus, loss modulus, and loss factor (tan delta) subjected to the PBS matrix composites were enhanced with untreated bamboo fiber and bamboo fiber treated with different concentrations of dopamine are shown in Figs. 8 and 9. In particular, the storage modulus was fairly sensitive to the bamboo fiber dispersion and interfacial interaction, as can be seen from the three DMA results (Zhou *et al*. 2013). As is shown in Fig. 8a, the storage modulus of the bamboo fiber/PBS composites exhibited a decreasing trend with increasing temperature, which is typical of thermoplastic matrix composites. Generally, the incorporation of a rigid filler (bamboo fiber) can improve the stiffness of the PBS matrix, which is represented by higher moduli values than for pure PBS (Chen *et al*. 2017b). However, when the filler had constant mass fractions and particle sizes, good interface bonding determined a high storage modulus value. Notably, the PDA treatment of the bamboo fiber in the PBS matrix-based composites induced a prominent increase in the storage modulus compared with the untreated group. For instance, at -60 °C, the storage modulus of the PDA-coated bamboo fiber/composites increased from 2503 (D-BF-5) to 2760 MPa (D-BF-2) for the bamboo fiber treated with different dopamine concentrations. Meanwhile, the untreated group only had a storage modulus value of 2262 MPa. These results indicated that the PDA-coated bamboo fiber was well distributed and had a compatible interface with the PBS matrix. Furthermore, the PDA loading rate was another factor related to the storage modulus, and the moderate loading content had the best properties, which was attributed to the strong interfacial adhesion between the fiber and matrix, as was discussed in the *Mechanical properties* section (pages 8429-8430). When the fibers were treated with a dopamine concentration of 1.0 mg/mL, the storage modulus of the composites reached its highest value (2760 MPa at -60 °C), which was 9.1% larger than that of D-BF-5 (dopamine concentration of 2.5 mg/mL), as well as 22.0% larger than that of the control.

Figure 8b depicts the loss modulus curves that were obtained for the composite samples. Over the whole temperature range, the temperature that corresponded to the peak of the loss modulus curve reflected the temperature of the polymer chains as they started to move or freeze, which is the glass transition temperature (T_g) (Gao *et al*. 2017). In this study, the increased T_g indicated there was a limitation to the growth of the PBS molecular chains. With the addition of PDA, the T_g was higher compared with the untreated group, which indicated that the PDA coating on the bamboo fiber delayed the segmentation of the PBS matrix, which was attributed to the compatible interface between the bamboo fiber and PBS matrix. Moreover, a single peak occurred in every loss modulus curve of the PBS matrix-based composite prepared from the bamboo fiber treated with PDA, which suggested that the incorporation of PDA may not have modified the original properties of the PBS molecular chains. This led to a good compatibility between the bamboo fiber and PBS. When the dopamine concentration was 1.0 mg/mL (D-BF-2), the storage modulus of the composites achieved its maximum value.

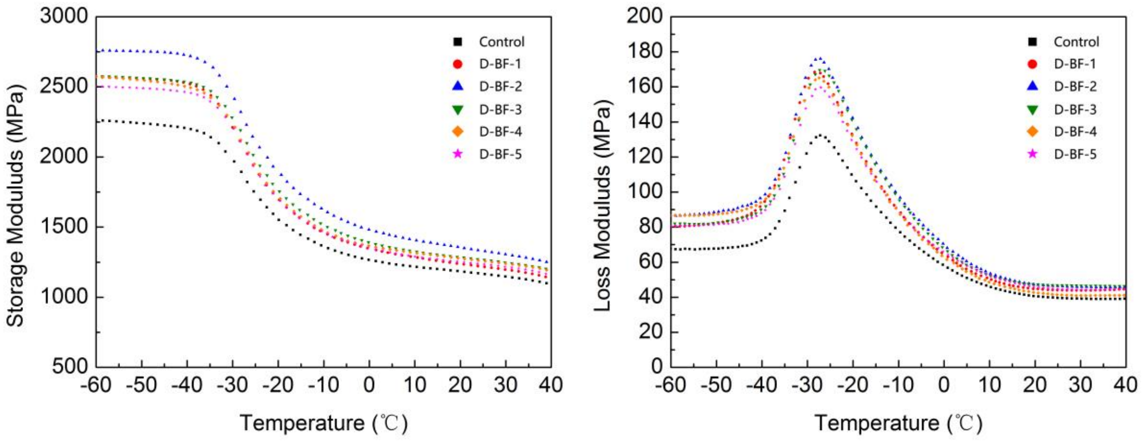

(a) **(b)**

Fig. 8. DMA curves of the bamboo fiber/PBS composites; (a) Storage modulus; (b) Loss modulus

Figure 9 shows the temperature dependence of the loss factor (tan delta) of the untreated and PDA-coated bamboo fiber/PBS composites. It was seen that the trend of the loss factor curve variation was the same as for the loss modulus, but the values of each curves were the opposite. Compared with the control group, utilizing PDA-treated bamboo fiber to prepare PBS matrix-based composites decreased the loss factor, and the minimum value was obtained with D-BF-2 (dopamine concentration of 1.0 mg/mL). The lower loss factor value generated a dissipation energy, which was attributed to the internal friction and molecular motion (Li *et al*. 2017). Kubát *et al*. (1990) found that strong interactions between the fiber and matrix at the interface tended to reduce the macromolecular mobility in the vicinity of the fiber surface compared with that in the bulk matrix. Therefore, the loss factor value had an important relationship with the interface compatibility. Herein, the adhesion factor (A) was used to evaluate the interfacial bonding with Eq. 2 at -26 °C. For example, in the experimental groups, the highest *A* values (0.177) occurred in D-BF-1, which represented the weakest interfacial interaction. The composite prepared from the bamboo fiber treated with a dopamine concentration of 1.0 mg/mL (D-BF-2) exhibited the strongest interactions with the lowest value of 0.042. The two values were both lower than that of the control group (0.234). This result proved that the PDA treatment of bamboo fiber improved the interfacial compatibility and that the best dopamine concentration was 1.0 mg/mL in this study.

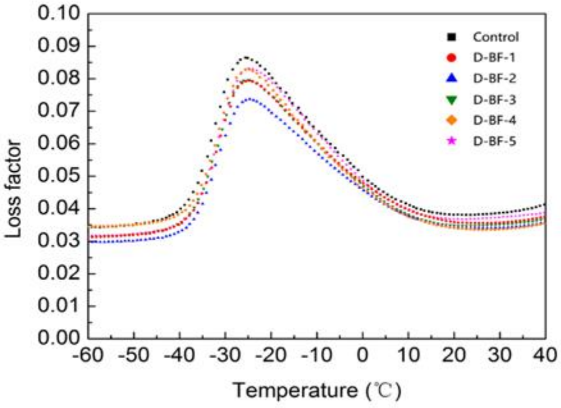

Fig. 9. Loss factor (tan delta) curves of the bamboo fiber/PBS composites

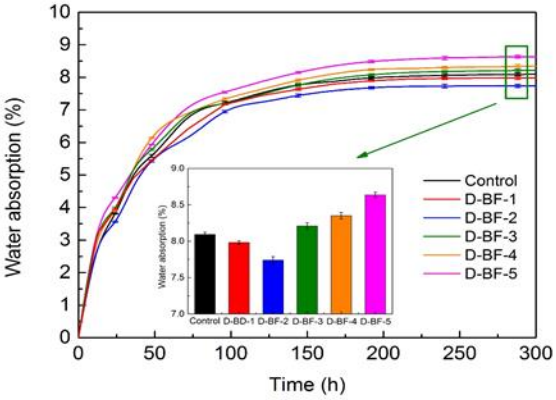

Fig. 10. Water absorption curves of the bamboo fiber/PBS composites

Water absorption capability

Figure 10 exhibits the water absorption (WA) capability of the various bamboo fiber/PBS composites. It was found that water uptake for all the samples increased apparently within the first 100 h, and then it slowed down and ultimately reached equilibrium. Due to the hydrophobic property of PBS that can absorb only the water of about 1% (Lee *et al*. 2013), the filling of the hydrophilic natural fiber and the related interfacial bonding performance will be the dominant factor influencing the WA of the composites. As shown in Fig. 10, the control group for the composites reinforced with plain bamboo fiber presented a higher WA capability with the final equilibrium moisture content (EMC) of 8.09%. This can be explained that the free hydroxyl groups in the fillers (bamboo fibers) can promote hydrogen bonding with water molecules, resulting in increasing the WA of the composites. Compared with the control group, the water resistance of the composites were slightly increased after incorporating the modified bamboo fiber with lower PDA loadings, and the minimum EMC values of 7.74% was observed in D-BF-2. This was probably due to the better interfacial bonding of bamboo fiber and PBS resin that reduced the existing gaps between the fiber and the matrix, which could limited the pathway for water within the composite (Najafi *et al*. 2007). However, with an increased dopamine concentration, the WA capability were found in D-BF-3, D-BF-4, and D-BF-5 with the values of 8.21%，8.35%，and 8.64%, respectively, which were all higher than the control one. This poor water resistance may be attributed to the accessible hydrophilic groups provided by the excess PDA nanoparticles that promoted the WA capability of the PDA coating substrate via hydrogen bonding, which was in accordance with the finding by Wang *et al*. (2017). In addition, as the poor interfacial bonding of these composites, the polar groups were more easily exposed to the water.

To sum up, although the appropriate loading rate of PDA can improve the interfacial bonding of the composite, the WA capability only decreased by 4.32% in D-BF-2, because the hydrogen bonding present at the interface between the modified bamboo fibers and PBS matrix was similar to PBS composites with plain fibers. Moreover, the water resistance performance became worse with the overloading rate of PDA nanoparticles. Hence, this mussel inspired modification method could not greatly reduced water absorption of the resultant bamboo fiber/PBS composites compared with the traditional compatibilizer such as silane (Haddou *et al.* 2016), and maleated coupling agents (Ren *et al.* 2017).

Surface morphology in SEM

Figure 11 shows the SEM micrographs of the fractured cross-section for the PBS matrix-based composites prepared from the untreated and PDA-treated bamboo fibers. The control group for the untreated bamboo fiber exhibited the worst fractured cross-section with a high roughness surface (Fig. 11a). There were many, regularly occurring holes with diameters larger than a single fiber. This effect was generated by the pull-out of agglomerated bamboo fibers. This result was attributed to the presence of free hydroxyl groups from the bamboo fiber, which made these fillers agglomerate, and thereby led to the inhibition of bamboo fiber dispersion in the PBS matrix and dramatically weakened the interaction between the two parts. The number of voids and agglomerated bamboo fibers on the impact fractured surface rapidly decreased, as shown in Figs. 11b to 11f, which suggested that the interfacial compatibility between the fillers and matrix was improved by the treatment of PDA nanoparticles, and different loading rates exhibited different enhancements. As shown in Fig. 10b, the lowest PDA loading rate on the bamboo fiber (D-BF-1) barely induced strong interactions between the fiber and PBS matrix. Consequently, the interface was easily broken down and voids appeared between the two components. With an increased dopamine concentration (D-BF-2, 1.0 mg/mL; D-BF-3, 1.5 mg/mL), the interfacial bonding was dramatically enhanced in the composites, which was shown in Figs. 11c and 11d. Figure 11c shows that a tightly integrated interface around single fibers was formed, and a good compatibility interface promoted uniform stress transmission, and thus bamboo fiber breakage occurred. Figure 11d also shows that the bamboo fibers were well wrapped in the PBS matrix because of the compatible interface and homogeneous filler dispersion. However, when the dopamine concentration continued to increase (D-BF-4, 2.0 mg/mL), a separate interface and large number of small holes appeared again, as can be seen in Fig. 11e. This phenomenon demonstrated that excess PDA increased the content of free hydroxyl groups, which weakened the interface interaction between the bamboo fiber and PBS matrix. Although agglomerated bamboo fibers were rarely spotted in the fractured cross-section, single bamboo fibers were frequently pulled out because of the relatively poor interfacial bonding, which left small voids irregularly distributed across the fractured surface. Furthermore, when the dopamine concentration increased to the highest level used in this study (D-BF-5, 2.5 mg/mL), the polarity of the bamboo fiber surface increased because of the presence of a large number of hydrophilic groups (-OH, -NH) provided by the excess PDA nanoparticles. The bamboo fibers agglomerated again, which was attributed to the hydrogen bonds formed with the hydrophilic groups of the PDA molecular chains. This induced the weakest interfacial bonding in the experimental groups, and a rougher fractured surface was observed in Fig. 11f. These findings were consistent with the mechanical test results, which indicated that an appropriate dopamine treatment solution concentration can remarkably improve the interfacial compatibility between the bamboo fiber and PBS matrix.

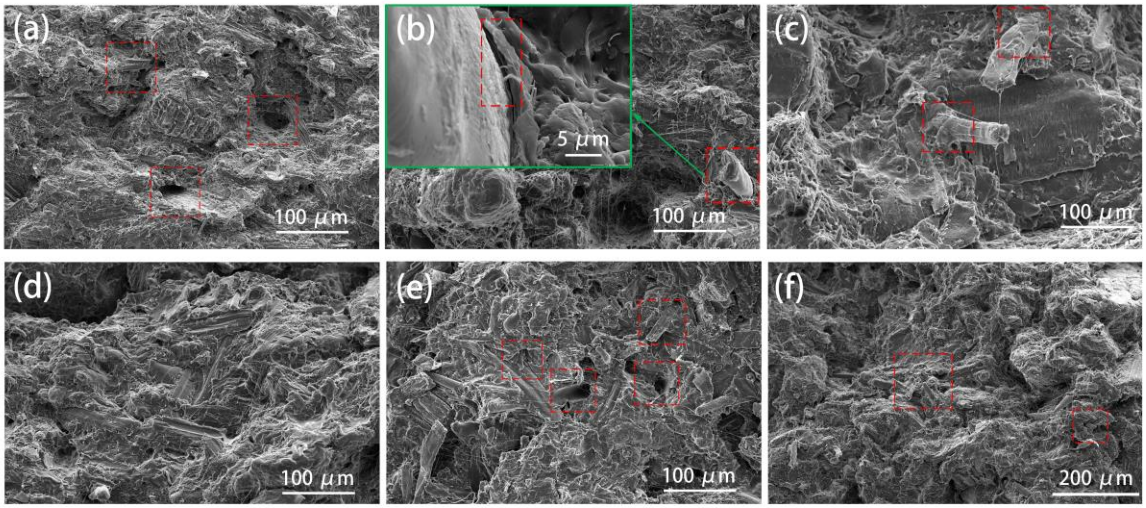

Fig. 11. SEM micrographs of the fractured cross-section of the PBS matrix-based composites prepared from the untreated and PDA-treated bamboo fibers; (a) Control; (b) D-BF-1; (C) D-BF-2; (d) D-BF-3; (e) D-BF-4; (f) D-BF-5

In brief, the bionic modification, which had the advantages of high efficiency, simple operation, and non-toxicity, made PDA a promising compatibilizer for biomass fiber/biodegradable plastic composites that can be used in furniture production and packaging applications.

CONCLUSIONS

1. Inspired by mussel adhesion proteins, an environmentally friendly and convenient method to modify bamboo fiber with PDA was developed. The successful coating of PDA onto the surface of the bamboo fiber was verified by the absorbance-FTIR analysis and AFM. With the process of self-polymerization, PDA was formed that was approximately 77 nm in size. At the optimum amount, these nanoparticles decreased the number of free hydroxyl groups *via* hydrogen bonding, which reduced the polarity of the bamboo fiber and led to a better compatibility between the filler and plastic matrix. The XRD analysis indicated that there was almost no change to the crystalline region in the cellulose chain.
2. To evaluate the effects of the bio-modification on the properties of the biomass fiber-reinforced polymer composites, bamboo fiber/PBS biocomposites were prepared from fiber treated with different concentrations of dopamine using compression molding. The PDA-loaded nanoparticles improved the interfacial bonding between the bamboo fiber and PBS matrix, which resulted in the dramatic enhancement of the mechanical properties, thermal stability, and storage modulus. However, the PDA loading rate had a significant influence on the enhancements. The lowest PDA loading rate hardly induced strong interactions between the fiber and PBS matrix, while the highest PDA loading rate made the bamboo fibers agglomerate because of the increased content of hydrophilic groups (-OH, -NH). This was confirmed in the SEM micrographs of the

fractured cross-sections. Furthermore, the DSC results showed that the nucleation ability of the bamboo fiber was promoted as the PDA loading rate increased. In addition, this novel modification method had little effect on the water resistance of the resultant PBS composites. Consequently, the best dopamine concentration in this study was 1.0 mg/mL, for which the flexural strength, flexural modulus, tensile strength, tensile modulus, and impact strength increased by 34.2%, 23.4%, 65.5%, 41.3%, and 63.4%, respectively, compared with the untreated composites.

ACKNOWLEDGMENTS

This study was supported by the “Co-built Foundation with Beijing Municipal Education Commission ‘R & D on Key Technology in Scientific Utilization of Non-wood Plant Raw Materials’”, “National Natural Science Foundation of China (Grant No. 31670571)”, “Beijing Natural Science Foundation (Grant No. 6162019)”, and “Co-built Foundation with Zhejiang Province ‘R & D on Natural Fiber Composites and Environmentally Friendly Adhesives (Grant No. CZXC201410)’”.

REFERENCES CITED

ASTM D790-03 (2003). “Standard test methods for flexural properties of unreinforced and reinforced plastics and electrical insulating materials,” ASTM International, West Conshohocken, USA. DOI: 10.1520/D0790-03

ASTM D638-03 (2003). “Standard test method for tensile properties of plastics,” ASTM International, West Conshohocken, USA. DOI: 10.1520/D0638-03

ASTM D256-03 (2003). “Standard test methods for determining the lzod pendulum impact resistance of plastics,” ASTM International, West Conshohocken, USA. DOI: 10.1520/D0256-03

Bourmaud, A., Riviere, J., Le Duigou, A., Raj, G., and Baley, C. (2009). "Investigations of the use of a mussel-inspired compatibilizer to improve the matrix-fiber adhesion of a biocomposite," *Polym. Test.* 28(6), 668-672. DOI: 10.1016/j.polymertesting.2009.04.006

Chen, F., Han, G., Li, Q., Gao, X., and Cheng, W. (2017a). "High-temperature hot air/silane coupling modification of wood fiber and its effect on properties of wood fiber/HDPE composites," *Materials* 10(3), 286-302. DOI: 10.3390/ma10030286

Chen, S., Cheng, L., Huang, H., Zou, F., and Zhao, H.-P. (2017b). "Fabrication and properties of poly(butylene succinate) biocomposites reinforced by waste silkworm silk fabric," *Compos. Part A-Appl. S.* 95, 125-131. DOI: 10.1016/j.compositesa.2017.01.004

Chu, J., Zhang, J.-h., Ma, L., and Lu, H.-d. (2017). "Study of crystallinity performance of pretreated bamboo fibers based on x-ray diffraction and NMR," *Spectrosc. Spect. Anal*. 37(1), 256-261. DOI: 10.3964/j.issn.1000-0593(2017)01-0256-06

Deming, T. J. (1999). "Mussel byssus and biomolecular materials," *Curr. Opin. Chem. Biol.* 3(1), 100-105. DOI: 10.1016/S1367-5931(99)80018-0

Gao, X., Li, Q., Cheng, W., Han, G., and Xuan, L. (2016). "Optimization of high temperature and pressurized steam modified wood fibers for high-density polyethylene matrix composites using the orthogonal design method," *Materials* 9(10), 847. DOI: 10.3390/ma9100847

Gao, X., Li, Q., Cheng, W., Han, G., and Xuan, L. (2017). "High temperature and pressurized steaming/silane coupling co-modification for wood fibers and its effect on the properties of wood fiber/HDPE composites," *Macromolecular Research* 25(2), 141-150. DOI: 10.1007/s13233-017-5024-x

Gu, C., Huang, X., Shi, M., Zhang, M., Wang, X.-L., and Zheng, Z. (2013). "Bio-inspired layer-by-layer assembled hybrid films for improvement of mechanical properties," *Polym. Composite.* 34(8), 1261-1268. DOI: 10.1002/pc.22536

Guo, D. (2017). "Effect of electron beam radiation processing on mechanical and thermal properties of fully biodegradable crops straw/poly (vinyl alcohol) biocomposites," *Radiat. Phys. Chem.* 130, 202-207. DOI: 10.1016/j.radphyschem.2016.08.024

Haddou, G., Dandurand, J., Dantras, E., Maiduc, H., Thai, H., Giang, N. V., Trung, T. H., Ponteins, P., and Lacabanne, C. (2016). "Mechanical and thermal behaviour of bamboo flour-reinforced XLPE composites," *J. Therm. Anal. Calorim.* 124(2), 701-708. DOI: 10.1007/s10973-015-5176-x

Hassaini, L., Kaci, M., Touati, N., Pillin, I., Kervoelen, A., and Bruzaud, S. (2017). "Valorization of olive husk flour as a filler for biocomposites based on poly(3-hydroxybutyrate-co-3-hydroxyvalerate): Effects of silane treatment," *Polym. Test.* 59, 430-440. DOI: 10.1016/j.polymertesting.2017.03.004

Ji, Y., Ji, T., Liang, K., and Zhu, L. (2016). "Mussel-inspired soft-tissue adhesive based on poly(diol citrate) with catechol functionality," *J. Mater. Sci.-Mater. M.* 27, 30. DOI: 10.1007/s10856-015-5649-2

Kim, H.-S., Kim, H.-J., Lee, J.-W., and Choi, I.-G. (2006). "Biodegradability of bio-flour filled biodegradable poly(butylene succinate) bio-composites in natural and compost soil," *Polym. Degrad. Stabil.* 91(5), 1117-1127. DOI: 10.1016/j.polymdegradstab.2005.07.002

Koronis, G., Silva, A., and Fontul, M. (2013). "Green composites: A review of adequate materials for automotive applications," *Compos. Part B-Eng.* 44(1), 120-127. DOI: 10.1016/j.compositesb.2012.07.004

Kubát, J., Rigdahl, M., and Welander, M. (1990). "Characterization of interfacial interactions in high density polyethylene filled with glass spheres using dynamic-mechanical analysis," *J. Appl. Polym. Sci.* 39(7), 1527-1539. DOI: 10.1002/app.1990.070390711

Lee, G. M., Oh, A. G., and An, S. K. (2016). "Effects of hexamethylene diisocyanate as coupling agent on mechanical properties of bamboo/PBS composites," *Textile Science and Engineering* 53(1), 36-44. DOI: 10.12772/TSE.2016.53.036

Lee, H., Dellatore, S. M., Miller, W. M., and Messersmith, P. B. (2007). "Mussel-inspired surface chemistry for multifunctional coatings," *Science* 318(5849), 426-430. DOI: 10.1126/science.1147241

Lee, J. M., Ishak, Z. A. M., Taib, R. M., Law, T. T., and Thirmizir, M. Z. A. (2013). "Mechanical, thermal and water absorption properties of kenaf-fiber-based polypropylene and poly(butylene succinate) composites," *J. Polym. Environ.* 21(1), 293-302. DOI: 10.1007/s10924-012-0516-4

Lee, S. M., Cho, D., Park, W. H., Lee, S. G., Han, S. O., and Drzal, L. T. (2005). "Novel silk/poly(butylene succinate) biocomposites: The effect of short fibre content on their mechanical and thermal properties," *Compos. Sci. Technol.* 65(3-4), 647-657.

DOI: 10.1016/j.compscitech.2004.09.023

Li, Q., Gao, X., Cheng, W., and Han, G. (2017). "Effect of modified red pottery clay on the moisture absorption behavior and weatherability of polyethylene-based wood-plastic composites," *Materials* 10(2), 111. DOI: 10.3390/ma10020111

Li, Y., Sang, L., Wei, Z., Ding, C., Chang, Y., Chen, G., Zhang, W., and Liang, J. (2015). "Mechanical properties and crystallization behavior of poly(butylene succinate) composites reinforced with basalt fiber," *J. Therm. Anal. Calorim.* 122(1), 261-270. DOI: 10.1007/s10973-015-4732-8

Liang, J., Ding, C., Wei, Z., Sang, L., Song, P., Chen, G., Chang, Y., Xu, J., and Zhang, W. (2015). "Mechanical, morphology, and thermal properties of carbon fiber reinforced poly(butylene succinate) composites," *Polym. Composite.* 36(7), 1335-1345. DOI: 10.1002/pc.23038

Lin, Q., Gourdon, D., Sun, C., Holten-Andersen, N., Anderson, T. H., Waite, J. H., and Israelachvili, J. N. (2007). "Adhesion mechanisms of the mussel foot proteins mfp-1 and mfp-3," *P. Natl. Acad. Sci. USA* 104(10), 3782-3786. DOI: 10.1073/pnas.0607852104

Liu, L., Yu, J., Cheng, L., and Qu, W. (2009). "Mechanical properties of poly(butylene succinate) (PBS) biocomposites reinforced with surface modified jute fibre," *Compos. Part A-Appl. S.* 40(5), 669-674. DOI: 10.1016/j.compositesa.2009.03.002

Liu, R., Peng, Y., Cao, J., and Chen, Y. (2014). "Comparison on properties of lignocellulosic flour/polymer composites by using wood, cellulose, and lignin flours as fillers," *Compos. Sci. Technol.* 103, 1-7. DOI: 10.1016/j.compscitech.2014.08.005

Liu, W., Xie, T., and Qiu, R. (2016). "Bamboo fibers grafted with a soybean-oil-based monomer for its unsaturated polyester composites," *Cellulose* 23(4), 2501-2513. DOI: 10.1007/s10570-016-0969-z

Luo, C., Zou, Z., Luo, B., Wen, W., Li, H., Liu, M., and Zhou, C. (2016). "Enhanced mechanical properties and cytocompatibility of electrospun poly(L-lactide) composite fiber membranes assisted by polydopamine-coated halloysite nanotubes," *Appl. Surf. Sci.* 369, 82-91. DOI: 10.1016/j.apsusc.2016.02.048

Matkó, S., Toldy, A., Keszei, S., Anna, P., Bertalan, G., and Marosi, G. (2005). "Flame retardancy of biodegradable polymers and biocomposites," *Polym. Degrad. Stabil.* 88(1), 138-145. DOI: 10.1016/j.polymdegradstab.2004.02.023

Matos-Pérez, C. R., White, J. D., and Wilker, J. J. (2012). "Polymer composition and substrate influences on the adhesive bonding of a biomimetic, cross-linking polymer," *J. Am. Chem. Soc.* 134(22), 9498-9505. DOI: 10.1021/ja303369p

Moustafa, H., Guizani, C., and Dufresne, A. (2017). "Sustainable biodegradable coffee grounds filler and its effect on the hydrophobicity, mechanical and thermal properties of biodegradable PBAT composites," *J. Appl. Polym. Sci.* 134(8). DOI: 10.1002/app.44498

Najafi, S. K., Kiaefar, A., Hamidina, E., and Tajvidi, M. (2007). "Water absorption behavior of composites from sawdust and recycled plastics," *J. Reinf. Plast. Comp.* 26(3), 341-348. DOI: 10.1177/0731684407072519

Ren, D., Yu, Z., Zhang, X., Wang, H., Wang, H., and Yu, Y. (2017). "Quantitative characterization of the interface between bamboo fiber and polypropylene with pull-out test and nanomechanical imaging," *J. Mater. Sci.* 52(3), 1296-1307. DOI: 10.1007/s10853-016-0425-3

Song, W., Zhao, F., Yu, X., Wang, C., Wei, W., and Zhang, S. (2015). "Interfacial characterization and optimal preparation of novel bamboo plastic composite engineering materials," *BioResources* 10(3), 5049-5070. DOI: 10.15376/biores.10.3.5049-5070

Tang, C.-M., Tian, Y.-H., and Hsu, S.-H. (2015). "Poly(vinyl alcohol) nanocomposites reinforced with bamboo charcoal nanoparticles: Mineralization behavior and characterization," *Materials* 8(8), 4895-4911. DOI: 10.3390/ma8084895

Thakur, V. K., Thakur, M. K., Raghavan, P., and Kessler, M. R. (2014). "Progress in green polymer composites from lignin for multifunctional applications: A review," *ACS Sustainable & Chemistry Engineering* 2(5), 1072-1092. DOI: 10.1021/sc500087z

Waite, J. H. (2008). "Surface chemistry - Mussel power," *Nature Materials* 7(1), 8-9. DOI: 10.1038/nmat2092

Wan, Q., Tian, J., Liu, M., Zeng, G., Li, Z., Wang, K., Zhang, Q., Deng, F., Zhang, X., and Wei, Y. (2015). "Mussel inspired preparation of highly dispersible and biocompatible carbon nanotubes," *RSC Advances* 5(32), 25329-25336. DOI: 10.1039/C4RA13408G

Wang, K. L., Dong, Y. M., Yan, Y. T., Zhang, S. F., and Li, J. Z. (2017). "Mussel-inspired chemistry for preparation of superhydrophobic surfaces on porous substrates." *RSC Advances.* 7(46), 29149-29158. DOI: 10.1039/c7ra04790h

Wang, W., Jiang, Y., Liao, Y., Tian, M., Zou, H., and Zhang, L. (2011). "Fabrication of silver-coated silica microspheres through mussel-inspired surface functionalization," *J. Colloid Interf. Sci.* 358(2), 567-574. DOI: 10.1016/j.jcis.2011.03.023

Wang, Z., Kang, H., Qi, C., Zhang, S., and Li, J. (2017). "Multiple cross-linking bionanocomposites reinforced with mussel-inspired poly(dopamine) surface modified nanoclay: Construction, properties, and characterization," *Polym. Composite.* DOI: 10.1002/pc.24365

Xie, Y., Hill, C. A. S., Xiao, Z., Militz, H., and Mai, C. (2010). "Silane coupling agents used for natural fiber/polymer composites: A review," *Compos. Part A-Appl. S.* 41(7), 806-819. DOI: 10.1016/j.compositesa.2010.03.005

Xu, X.-l., Zhang, M., Qiang, Q., Song, J.-q., and He, W.-q. (2016). "Study on the performance of the acetylated bamboo fiber/PBS composites by molecular dynamics simulation," *J. Compos. Mater.* 50(7), 995-1003. DOI: 10.1177/0021998315615690

Yang, L., Phua, S. L., Teo, J. K. H., Toh, C. L., Lau, S. K., Ma, J., and Lu, X. (2011). "A biomimetic approach to enhancing interfacial interactions: Polydopamine-coated clay as reinforcement for epoxy resin," *ACS Applied Materials & Interfaces* 3(8), 3026-3032. DOI: 10.1021/am200532j

Yao, L., Wang, Y., Li, Y., and Duan, J. (2017). "Thermal properties and crystallization behaviors of polylactide/redwood flour or bamboo fiber composites," *Iran. Polym. J.* 26(2), 161-168. DOI: 10.1007/s13726-017-0508-2

Yuan, J., Zhang, Z., Yang, M., Guo, F., Men, X., and Liu, W. (2017). "Surface modification of hybrid-fabric composites with amino silane and polydopamine for enhanced mechanical and tribological behaviors," *Tribol. Int.* 107, 10-17. DOI: 10.1016/j.triboint.2016.11.013

Zhang, X., Wang, F., and Keer, L. (2015). "Influence of surface modification on the microstructure and thermo-mechanical properties of bamboo fibers," *Materials* 8(10), 6597-6608. DOI: 10.3390/ma8105327

Zhang, Y., Yu, C., Chu, P. K., Lv, F., Zhang, C., Ji, J., Zhang, R., and Wang, H. (2012). "Mechanical and thermal properties of basalt fiber reinforced poly(butylene succinate) composites," *Mater. Chem. Phys.* 133(2-3), 845-849. DOI: 10.1016/j.matchemphys.2012.01.105

Zhou, M., Li, Y., He, C., Jin, T., Wang, K., and Fu, Q. (2014a). "Interfacial crystallization enhanced interfacial interaction of poly (butylene succinate)/ramie fiber biocomposites using dopamine as a modifier," *Compos. Sci. Technol.* 91, 22-29. DOI: 10.1016/j.compscitech.2013.11.019

Zhou, M., Xu, S., Li, Y., He, C., Jin, T., Wang, K., Deng, H., Zhang, Q., Chen, F., and Fu, Q. (2014b). "Transcrystalline formation and properties of polypropylene on the surface of ramie fiber as induced by shear or dopamine modification," *Polymer* 55(13), 3045-3053. DOI: 10.1016/j.polymer.2014.05.013

Zhou, M., Yan, J., Li, Y., Geng, C., He, C., Wang, K., and Fu, Q. (2013). "Interfacial strength and mechanical properties of biocomposites based on ramie fibers and poly(butylene succinate)," *RSC Advances* 3(48), 26418-26426. DOI: 10.1039/C3RA43713B

Article submitted: June 13, 2017; Peer review completed: August 18, 2017; Revised version received and accepted: September 10, 2017; Published: September 25, 2017.
DOI: 10.15376/biores.12.4.8419-8442